

Modeling of an FAU-type zeolite membrane reactor for the catalytic dehydrogenation of cyclohexane

Byeong-Heon Jeong, Ken-Ichiro Sotowa, Katsuki Kusakabe*

Department of Applied Chemistry, Kyushu University, Fukuoka 812-8581, Japan

Received 27 October 2003; accepted 23 March 2004

Abstract

A simple mathematical model assuming isothermal operation and a plug flow pattern was developed to evaluate the performance of an FAU-type zeolite membrane reactor for use in the catalytic dehydrogenation of cyclohexane. The membrane reactor consisted of a catalyst bed and membrane, containing an impermeable region at the reactor inlet, followed by a permeable region. The impermeable region was required in order to achieve an equilibrium conversion before entering the permeable region, and the selective permeation of benzene and hydrogen was sufficient to shift the equilibrium. The results of the simulation for the membrane reactor were in good agreement with the experimental results. On the basis of the simulation, the zeolite membrane reactor was superior to the Knudsen membrane reactor. The effect of co-feeding hydrogen with cyclohexane, to restrain coke formation on the catalyst due to the high hydrogen concentration in the feed side was clearly demonstrated. The effect of permeance and the separation factor on the conversion was evaluated, and as a result, the permeance was more important in terms of increasing the conversion than the separation factor.

© 2004 Elsevier B.V. All rights reserved.

Keywords: Modeling; Simulation; Membrane reactor; FAU-type zeolite; Dehydrogenation; Cyclohexane

1. Introduction

Zeolite membranes are of interest for a membrane reactor system because of their desirable thermal properties and high hydrogen permeability [1–4]. Although palladium-based membranes have an infinite selectivity for hydrogen permeation, which is suitable for dehydrogenation, they are poisoned by sulfur impurities in the feed side [5], deactivated by coking in dehydrogenation reactions [6], and eventually fail [7].

To evaluate the performance of a membrane reactor, a number of modeling studies have been conducted. Most of the models are concerned with equilibrium-limited reactions since these systems have been mostly studied experimentally [3,4,8–10]. The dehydrogenation of cyclohexane has been extensively studied as a model reaction in various membrane

reactors [11–15].



Itoh and coworkers [11,12] experimentally and theoretically studied this reaction using a microporous Vycor glass membrane reactor and a palladium membrane reactor. Cyclohexane in the feed side was diluted with an inert gas and a sweep gas was introduced to the permeate side. A mathematical model assuming plug flow and isothermal conditions was developed. An increase in the flow rate of the sweep gas led to a decrease in the concentration of hydrogen in the permeate side. This resulted in an increase in the driving force for diffusion through the membrane, thus increasing the conversion. As the flow rate in the feed side decreased, the residence time in the reactor increased, and consequently the conversion increased. It should be noted that excellent agreement between the model and the experimental data was reported.

Kokugan et al. [13] fed pure cyclohexane directly into the feed side of membrane reactors. The conversions in the membrane reactors were evaluated using the pseudo equilibrium

* Corresponding author. Tel.: +81 92 642 3552; fax: +81 92 651 5606.
E-mail address: kusactf@mbox.nc.kyushu-u.ac.jp (K. Kusakabe).

Nomenclature

k	apparent reaction rate constant ($\text{mol m}^{-3} \text{Pa}^{-1} \text{s}^{-1}$)
K_B	adsorption equilibrium constant of benzene (Pa^{-1})
K_p	equilibrium constant (Pa^3)
l	distance from the inlet of the reactor (m)
L	length of reactor (m)
$N_{i,F}$	molar flow rate of component i in the feed side (mol s^{-1})
$N_{i,P}$	molar flow rate of component i in the permeate side (mol s^{-1})
p_i	partial pressure of component i in the feed side (Pa)
P_F	total feed pressure (Pa)
P_P	total permeate pressure (Pa)
Q_i	permeance of component i ($\text{mol m}^{-2} \text{s}^{-1} \text{Pa}^{-1}$)
r	outer radius of the porous support tube (m)
r_C	dehydrogenation rate of cyclohexane ($\text{mol m}^{-3} \text{s}^{-1}$)
R	gas constant ($\text{m}^3 \text{Pa mol}^{-1} \text{K}^{-1}$)
S_R	cross-sectional area of catalyst bed (m^2)
$u_{x,0}$	gas flow rate at the inlet of the feed side ($\text{m}^3 \text{s}^{-1}$)
$u_{x,1}$	gas flow rate at the outlet of the feed side ($\text{m}^3 \text{s}^{-1}$)
$u_{y,0}$	gas flow rate at the inlet of the permeate side ($\text{m}^3 \text{s}^{-1}$)
$u_{y,1}$	gas flow rate at the outlet of the permeate side ($\text{m}^3 \text{s}^{-1}$)
V_F	total feed flow rate ($\text{m}^3 \text{s}^{-1}$)
V_P	total permeate flow rate ($\text{m}^3 \text{s}^{-1}$)
V_R	gross volume of reaction section (m^3)
x_i	mole fraction of component i in the feed side
$x_{i,0}$	mole fraction of component i at the inlet of the feed side
$x_{i,1}$	mole fraction of component i at the outlet of the feed side
X_C	conversion of cyclohexane
y_i	mole fraction of component i in the permeate side
$y_{i,0}$	mole fraction of component i at the inlet of the permeate side
$y_{i,1}$	mole fraction of component i at the outlet of the permeate side

Greek letters

$\alpha(i/j)$	separation factor of component i to component j
ν_i	stoichiometric coefficient of component i

Subscripts

A	argon
B	benzene
C	cyclohexane
H	hydrogen
i	component i
j	component j

model, derived from the Gibb's free energy change for the reaction and the equilibrium constant. The predicted conversions using the pseudo equilibrium model were also in good agreement with the experimental data.

A pseudo-homogeneous model was recently used to describe the transport mechanism through a catalyst bed [14,15]. Radial diffusion and/or axial diffusion were considered to account for the concentration gradient in the radial direction, due to the selective permeation of hydrogen through the membrane. They defined the optimal configurations for various conditions for a given reactor geometry.

In a previous paper [16], the catalytic dehydrogenation of cyclohexane in an FAU-type zeolite membrane reactor was examined and an increase in conversion in the membrane reactor, exceeding the equilibrium value, was achieved, as the result of the simultaneous removal of benzene and hydrogen. The permeation properties of benzene and cyclohexane through an FAU-type zeolite membrane have been reported in detail [17,18]. The contribution of the permeation properties of benzene and hydrogen to the conversion, however, is not still clear. The co-feeding hydrogen with cyclohexane to the feed side can also be tolerated in this system.

In the present study, we report on the development of a simple mathematical model assuming isothermal operation and a plug flow pattern, in an evaluating of the performance of an FAU-type zeolite membrane reactor for use in the catalytic dehydrogenation of cyclohexane and the simulation results are compared with experimental data [16]. The effect of co-feeding hydrogen with cyclohexane to the feed side on conversion is evaluated, and the relationship between the permeance and the separation factor is discussed.

2. Mathematical model

A simple mathematical model was developed to evaluate the performance of an FAU-type zeolite membrane reactor for the catalytic dehydrogenation of cyclohexane under the following assumptions:

- (1) isothermal conditions;
- (2) plug flow in both the feed and permeate sides;
- (3) no axial or radial diffusion;
- (4) permeation through the membrane is proportional to the difference in partial pressures between the feed and permeate sides;

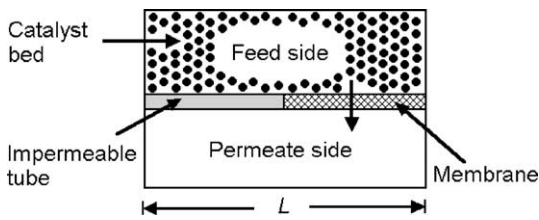


Fig. 1. Schematic diagram of a zeolite membrane reactor.

- (5) dehydrogenation reactions take place only on the catalysts packed in the feed side.

The simulated membrane reactor was composed of a quartz glass tube (i.d. = 10 mm, o.d. = 13 mm) containing an FAU-type zeolite membrane, which was fixed coaxially in the tubular reactor, as illustrated in Fig. 1. Almost half of the catalyst was packed in the area upstream from the permeation portion. The cyclohexane was diluted with argon and fed to the catalyst bed in the feed side of the membrane. Pure argon was also introduced to the permeate side of the membrane as a sweep gas. The total pressure in both the feed and permeate sides was maintained at 101.3 kPa. The model parameters for simulation are summarized in Table 1.

The mass balance equations for component i in the feed side and the permeate side in the membrane reactor are given as follows:

Feed side (catalyst bed):

$$\frac{dN_{i,F}}{dl} = v_i r_C S_R - 2\pi r Q_i (P_F x_i - P_P y_i) \quad (2)$$

Table 1
Parameters used in the simulation of a zeolite membrane reactor

Membrane	
Inner radius (m)	0.85×10^{-3}
Outer radius (m)	1.05×10^{-3}
Length (m)	2.65×10^{-2}
Reactor	
Length (L) (m)	6.00×10^{-2}
Inner radius of shell (m)	5.00×10^{-3}
Catalyst bed	
Cross-sectional area (S_R) (m ²)	7.50×10^{-5}
Feed side	
Total flow rate (V_F) (m ³ s ⁻¹)	3.34×10^{-7}
Total pressure (P_F) (Pa)	1.013×10^5
Mole fraction of C ($x_{C,0}$)	0.10
Mole fraction of A ($x_{A,0}$)	0.90
Permeate side	
Total flow rate (V_P) (m ³ s ⁻¹)	1.67×10^{-6}
Total pressure (P_P) (Pa)	1.013×10^5
Mole fraction of C ($y_{C,0}$)	0.00
Mole fraction of A ($y_{A,0}$)	1.00
Permeance (Q_i) ^a	
Cyclohexane (Q_C) (mol m ⁻² s ⁻¹ Pa ⁻¹)	Variable
Benzene (Q_B) (mol m ⁻² s ⁻¹ Pa ⁻¹)	Variable
Hydrogen (Q_H) (mol m ⁻² s ⁻¹ Pa ⁻¹)	Variable
Argon (Q_A) (mol m ⁻² s ⁻¹ Pa ⁻¹)	1.00×10^{-10}

^a The permeance to each component is taken from Jeong et al. [16].

Permeate side:

$$\frac{dN_{i,P}}{dl} = 2\pi r Q_i (P_F x_i - P_P y_i) \quad (3)$$

where N_i is the molar flow rate of component i . l is the distance from the inlet of the reactor. v_i is the stoichiometric coefficient of component i . r_C is the dehydrogenation rate of cyclohexane. S_R is the cross-sectional area of catalyst bed. r is the outer radius of the porous support tube. Q_i is the permeance of component i . P_F and P_P are the total feed and permeate pressures. x_i and y_i are the mole fractions of component i in the feed and permeate sides, respectively.

3. Experiments and simulations

The following reaction rate equation of cyclohexane, r_C , was used [12]:

$$r_C = \frac{-k(K_P p_C / p_H^3 - p_B)}{1 + (K_B K_P p_C / p_H^3)} \quad (4)$$

where k , K_B , and K_P are, respectively, the reaction rate constant, the adsorption equilibrium constant for benzene, and the reaction equilibrium constant. p_i is the partial pressure of component i .

The dehydrogenation of cyclohexane was performed in a packed bed reactor 0.01 m in i.d. and 0.01 m in length with 1.0 wt.% Pt/Al₂O₃ particles sized between 149 and 210 μm in order to determine the reaction rate constant. At 673 K, prior to the reaction, the catalyst was treated with 20% O₂ diluted in argon for 3 h in order to remove any adsorbed species, and reduction of the catalyst was then carried out with 20% H₂ diluted in argon for 3 h. The vaporized cyclohexane was diluted with argon and fed to the catalyst bed, and the reaction then started. The reaction temperature was in the range of 430–470 K. The total pressure and the total flow rate in the reactor were maintained at 101.3 kPa and 1.67×10^{-6} m³ s⁻¹ throughout the experiments, respectively. The compositions at both the inlet and the outlet were analyzed by means of a gas chromatograph (Shimadzu GC-8A) equipped with a flame ionization detector for hydrocarbons and a thermal conductivity detector for hydrogen.

The literature values for K_B and K_P [12] could be successfully utilized in these experiments. The reaction rate constants as a function of temperature were fit to an Arrhenius plot, as shown in Fig. 2. The activation energy of 32 kJ mol⁻¹ was similar to that reported by Itoh et al. [19]. As a result, the reaction rate constant, k , was obtained as follows:

- $K_P = (4.89 \times 10^{35}) \exp(3.190/T)$ (Pa³).
- $K_B = (2.03 \times 10^{-10}) \exp(6.270/T)$ (Pa⁻¹).
- $k = 0.44 \exp(-3850/T)$ (mol m⁻³ Pa⁻¹ s⁻¹).

The model equations were numerically solved by the simplest Euler method using the above parameters. The conversion of cyclohexane, X_C , was calculated from the ratio of the molar fractions of cyclohexane at the outlets of the feed and

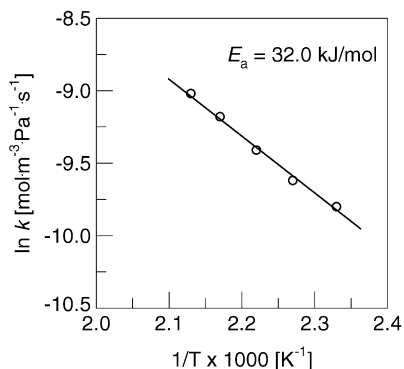


Fig. 2. Temperature dependency of the rate constant k .

the permeate sides to those for cyclohexane at the inlets of both sides as follows:

$$X_C = 1 - \frac{u_{x,1}x_{C,1} + u_{y,1}y_{C,1}}{u_{x,0}x_{C,0} + u_{y,0}y_{C,0}} \quad (5)$$

where $u_{x,0}$ and $u_{x,1}$ are the gas flow rates at the inlet and the outlet of the feed side, respectively. $u_{y,0}$ and $u_{y,1}$ are the gas flow rates at the inlet and the outlet of the permeate side, respectively.

4. Simulation results and discussion

4.1. Comparison of the model to experiments

Fig. 3 shows the changes in mole fraction of cyclohexane in the feed side as a function of distance from the reactor inlet. The simulations were performed at 423, 448, 473, and 498 K using the zeolite membrane reactor. The length of the impermeable region was 0.0335 m from the inlet of the feed side. For the simulations of the impermeable region (i.e., a packed bed reactor segment), the reaction term in the model equation was only considered by substituting Q_i in the permeation term with 0. Meanwhile, both reaction and permeation terms

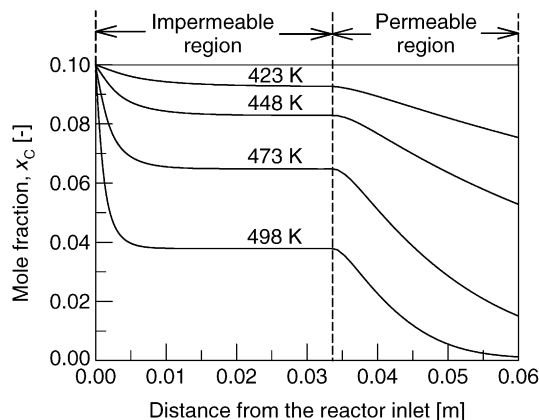


Fig. 3. Changes in the mole fraction of cyclohexane on the feed side as a function of distance from the reactor inlet. The permeances at each temperature were taken from Jeong et al. [16].

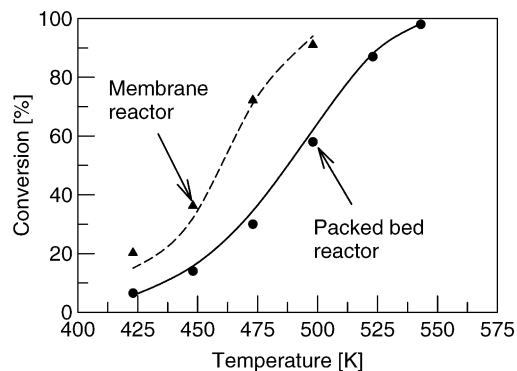


Fig. 4. Comparison between experimental and simulated results as a function of reaction temperature. (▲, ●) Experimental values; (---) simulated values; (—) thermodynamic equilibrium curve; feed rate of cyclohexane = $3.34 \times 10^{-8} \text{ m}^3 \text{ s}^{-1}$. The permeances at each temperature were taken from Jeong et al. [16].

were taken into account for the simulations of the permeable region (i.e., a membrane reactor segment). The mole fraction of cyclohexane decreased and was close to the equilibrium value at the end of impermeable region. A further decrease in cyclohexane concentration occurred in the permeable region, mainly due to the reaction resulting from a shift in the equilibrium. Consequently, the magnitude of the conversions at the end of the membrane reactor was much higher than the equilibrium values.

Fig. 4 shows a comparison between the experimental results [16] and the simulated ones as a function of reaction temperature. The total feed and permeate flow rates were 3.34×10^{-7} and $1.67 \times 10^{-6} \text{ m}^3 \text{ s}^{-1}$, respectively. The permeances to benzene, cyclohexane and hydrogen, which were experimentally determined using an FAU-type zeolite membrane for ternary mixtures [16], were used for the simulations. For the case of argon, however, permeation rate was extremely small and not able to be determined. Thus, the permeance to argon was assumed to be $1.0 \times 10^{-10} \text{ mol m}^{-2} \text{ s}^{-1} \text{ Pa}^{-1}$. The separation factors for hydrogen over cyclohexane were close to the Knudsen diffusion values, while the separation factors for benzene over cyclohexane were two or three times higher than those for hydrogen over cyclohexane [16]. The conversion in the zeolite membrane reactor could be successfully increased beyond the thermodynamic equilibrium value, which appears to be due to the simultaneous removal of benzene and hydrogen from the feed side of the membrane [16]. Good agreement was found between the simulated and the experimental values.

4.2. Effect of selective permeation properties of benzene and hydrogen

To evaluate the effect of the selective permeation of benzene on conversion in an FAU-type zeolite membrane reactor, the simulation of a membrane reactor (hereafter, referred to as a Knudsen membrane reactor) with a membrane showing Knudsen diffusion behavior, was carried out.

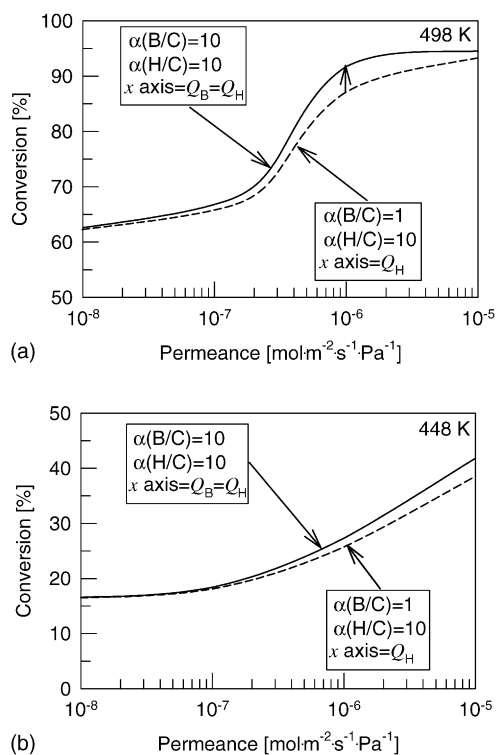


Fig. 5. Conversions calculated using the zeolite membrane reactor (solid line) and the Knudsen membrane reactor (dashed line) as a function of hydrogen permeance at (a) 498 K and (b) 448 K, respectively.

Fig. 5a and b shows the calculated conversions for the zeolite membrane reactor (solid line) and the Knudsen membrane reactor (dashed line) as a function of hydrogen permeance at 498 and 448 K, respectively. At a permeation rate of $1 \times 10^{-6} \text{ mol m}^{-2} \text{ s}^{-1} \text{ Pa}^{-1}$, the conversion in the zeolite membrane reactor was approximately 5% and 2% higher than that in the Knudsen membrane reactor at 498 and 448 K, respectively. As can be known in Fig. 5a and b, the increase in the conversion was largely affected by the selective permeation of hydrogen than that of benzene. Okubo et al. [20] reported on the dehydrogenation of cyclohexane in a membrane reactor with a thin γ -alumina membrane, which indicated Knudsen diffusion properties. The conversions in the Knudsen membrane reactor exceeded the equilibrium conversion.

4.3. Effect of co-feeding hydrogen with cyclohexane

When the dehydrogenation was performed in the membrane reactor with hydrogen selective membranes, coking on the catalyst, due to the lack of hydrogen, gradually decreased the conversion [7,21–23]. In the FAU-type zeolite membrane reactor, on the other hand, the co-feeding of hydrogen with cyclohexane to the reaction side is possible. Fig. 6a shows the influence of mole fraction of hydrogen at the inlet of the feed side on the conversion at 473 K. The mole fraction of cyclohexane at the inlet of the feed side was maintained at 0.1 and the permeation rate of hydrogen was fixed to $2 \times$

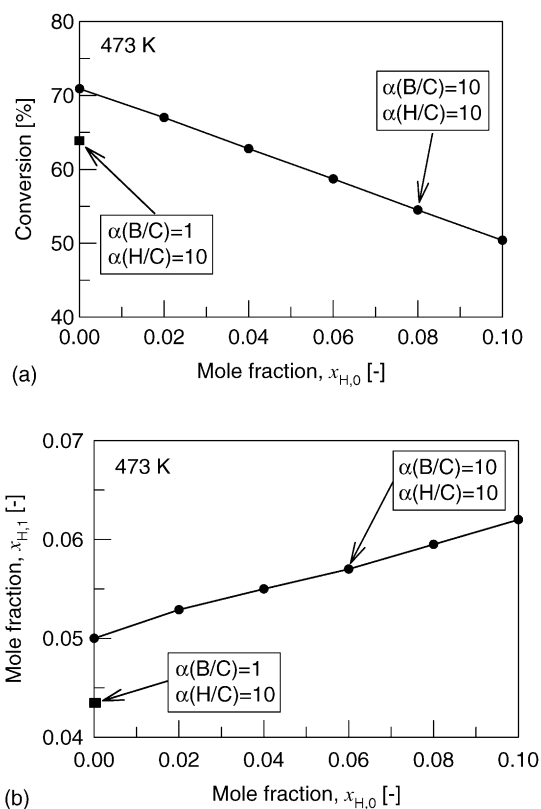


Fig. 6. Influence of the mole fraction of hydrogen at the inlet of the feed side on (a) conversion and (b) mole fraction of hydrogen at the outlet of the feed side at 473 K. The mole fraction of cyclohexane at the inlet of the feed side was maintained at 0.1. The hydrogen permeance was fixed to $2 \times 10^{-6} \text{ mol m}^{-2} \text{ s}^{-1} \text{ Pa}^{-1}$.

$10^{-6} \text{ mol m}^{-2} \text{ s}^{-1} \text{ Pa}^{-1}$. The conversion decreased with increasing mole fraction of hydrogen at the inlet. The mole fraction of hydrogen at the outlet of the feed side increased with increasing the mole fraction of hydrogen at the inlet of the feed side, as shown in Fig. 6b. The closed square symbols in Fig. 6a and b indicate the conversion and the mole fraction of hydrogen calculated for the Knudsen membrane reactor, respectively. The co-feeding hydrogen with cyclohexane into the zeolite membrane reactor permits the hydrogen concentration on the reaction side to be maintained, thus inhibiting the extent of coking. This may be the most useful feature of the zeolite membrane reactor, compared to a membrane reactor containing a hydrogen selective porous ceramic membrane.

4.4. Effect of the permeance and the separation factor

Fig. 7a and b show the changes in conversion calculated for the zeolite membrane reactor as a function of the permeance to benzene and hydrogen at 498 and 448 K, respectively. The solid circles indicate the experimental data for the zeolite membrane reactor. The conversion significantly increased with increasing permeance. Meanwhile, the

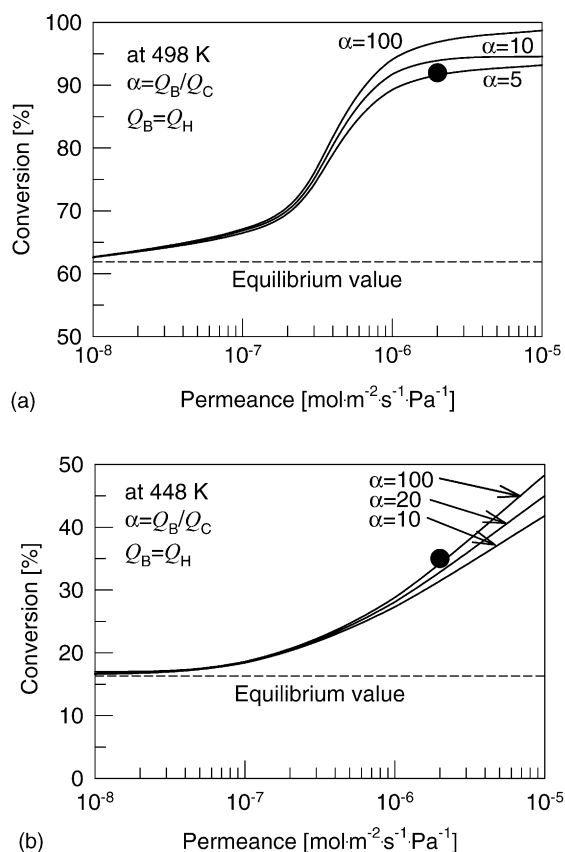


Fig. 7. Conversions calculated using the zeolite membrane reactor as a function of permeance to benzene and hydrogen at (a) 498 K and (b) 448 K, respectively.

conversion was changed only slightly as the separation factor increased. Thus, it can be concluded that the increase in conversion is mainly dependent on the permeance, rather than the separation factor. This conclusion is quite different compared to previously reported results [15,24], in which the separation factor is considered to be more important than permeance in a membrane reactor. Itoh and Haraya [25] examined a carbon membrane reactor for dehydrogenation, in which the membrane showed a molecular-sieving like diffusion behavior. For a binary system of hydrogen and cyclohexane, the permeance to hydrogen in the membrane was $2.0 \times 10^{-7} \text{ mol m}^{-2} \text{ s}^{-1} \text{ Pa}^{-1}$, which was approximately ten times lower than that in the zeolite membrane, and the separation factor for hydrogen over cyclohexane was 730 at 468 K. As a result, the carbon membrane reactor showed an increase in conversion comparable to the zeolite membrane reactor.

Thus, the permeance and the separation factor of a membrane should be optimized together for the optimal performance of a membrane reactor although the two factors have a trade-off relationship. From the view point of industrial applications, situations can arise where a high permeability in combination with a moderate selectivity is a better alternative to a high selectivity with a low permeability.

5. Conclusions

The catalytic dehydrogenation of cyclohexane in an FAU-type zeolite membrane reactor was simulated using a simple mathematical model, which was developed under the assumptions of isothermal operation and a plug flow pattern. The length of the impermeable region in the membrane reactor was found to be sufficient to permit an equilibrium conversion, and the selective permeation of benzene and hydrogen was effective in shifting the equilibrium. The conversion in the zeolite membrane reactor was much higher than the equilibrium conversion, and good agreement was found between the calculated values and the experimental ones. Based on the simulation results, the zeolite membrane reactor showed a better performance than the Knudsen membrane reactor. The co-feeding of hydrogen with cyclohexane into the reaction side, to prevent coking of the catalyst was effective. This can be attributed to the high hydrogen concentration on the reaction side. The increase in conversion in the zeolite membrane reactor was more dependent on the permeance than the separation factor.

Acknowledgements

This work was supported by the Japan Society for the Promotion of Science (JSPS) and the New Energy and Industrial Technology Development Organization (NEDO) of Japan. We also sincerely acknowledge the support of the NOK Corporation, Japan and the Tosoh Corporation, Japan.

References

- [1] M.P. Bernal, J. Coronas, M. Menéndez, J. Santamaría, Coupling of reaction and separation at the microscopic level: esterification processes in a H-ZSM-5 membrane reactor, *Chem. Eng. Sci.* 57 (2002) 1557–1562.
- [2] M.A. Salomón, J. Coronas, M. Menéndez, J. Santamaría, Synthesis of MTBE in zeolite membrane reactors, *Appl. Catal. A* 200 (2000) 201–210.
- [3] D. Casanave, P. Ciavarella, K. Fiati, J.-A. Dalmon, Zeolite membrane reactor for isobutane dehydrogenation: experimental results and theoretical modelling, *Chem. Eng. Sci.* 54 (1999) 2807–2815.
- [4] P. Ciavarella, H. Moueddeb, S. Miachon, K. Fiati, J.-A. Dalmon, Experimental study and numerical simulation of hydrogen/isobutene permeation and separation using MFI-zeolite membrane reactor, *Catal. Today* 56 (2000) 253–264.
- [5] Y.V. Gokhale, R.D. Noble, J.L. Falconer, Effects of reactant loss and membrane selectivity on a dehydrogenation reaction in a membrane-enclosed catalytic reactor, *J. Membr. Sci.* 105 (1995) 63–70.
- [6] S.H. Jung, K. Kusakabe, S. Morooka, S.-D. Kim, Effects of co-existing hydrocarbons on hydrogen permeation through a palladium membrane, *J. Membr. Sci.* 170 (2000) 53–60.
- [7] J.P. Collins, R.W. Schwartz, R. Sehgal, T.L. Ward, C.J. Brinker, G.P. Hagen, C.A. Udovich, Catalytic dehydrogenation of propane in hydrogen permselective membrane reactors, *Ind. Eng. Chem. Res.* 35 (1996) 4398–4405.
- [8] J.L. Falconer, R.D. Noble, D.P. Sperry, Catalytic membrane reactors, in: R.D. Noble, S.A. Stern (Eds.), *Membrane Separations Technol-*

- ogy: Principles and Applications, Elsevier, Amsterdam, 1995, pp. 669–712.
- [9] S. Assabumrungrat, J. Phongpatthanapanich, P. Praserttham, T. Tagawa, S. Goto, Theoretical study on the synthesis of methyl acetate from methanol and acetic acid in pervaporation membrane reactors: effect of continuous-flow modes, *Chem. Eng. J.* 95 (2003) 57–65.
- [10] J.M. Sousa, A. Mendes, Simulation study of a dense polymeric catalytic membrane reactor with plug-flow pattern, *Chem. Eng. J.* 95 (2003) 67–81.
- [11] N. Itoh, Y. Shindo, K. Haraya, T. Hakuta, A membrane reactor using microporous glass for shifting equilibrium of cyclohexane dehydrogenation, *J. Chem. Eng. Jpn.* 21 (1988) 399–404.
- [12] N. Itoh, A membrane reactor using palladium, *AIChE J.* 33 (1987) 1576–1578.
- [13] T. Kokugan, A. Trianto, H. Takeda, Dehydrogenation of pure cyclohexane in the membrane reactor and prediction of conversion by pseudo equilibrium model, *J. Chem. Eng. Jpn.* 31 (1998) 596–603.
- [14] A.M. Mondal, S. Ilias, Dehydrogenation of cyclohexane in a palladium–ceramic membrane reactor by equilibrium shift, *Sep. Sci. Technol.* 36 (2001) 1101–1116.
- [15] W.S. Moon, S.B. Park, S.-M. Yang, Optimal design conditions for dehydrogenation of cyclohexane in a membrane reactor, *Korean J. Chem. Eng.* 15 (1998) 136–140.
- [16] B.-H. Jeong, K.-I. Sotowa, K. Kusakabe, Catalytic dehydrogenation of cyclohexane in an FAU-type zeolite membrane reactor, *J. Membr. Sci.* 224 (2003) 151–158.
- [17] B.-H. Jeong, Y. Hasagawa, K. Kusakabe, S. Morooka, Separation of benzene and cyclohexane mixtures using an NaY-type zeolite membrane, *Sep. Sci. Technol.* 37 (2002) 1225–1239.
- [18] B.-H. Jeong, Y. Hasagawa, K.-I. Sotowa, K. Kusakabe, S. Morooka, Permeation of binary mixtures of benzene and saturated C₄–C₇ hydrocarbons through an FAU-type zeolite membrane, *J. Membr. Sci.* 213 (2003) 115–124.
- [19] N. Itoh, H. Tababe, Y. Shindo, T. Hakuta, Kinetic analysis of cyclohexane dehydrogenation over platinum catalyst, *Sekiyu Gakkaishi* 28 (1985) 323–327.
- [20] T. Okubo, K. Haruta, K. Kusakabe, S. Morooka, H. Anzai, S. Akiyama, Equilibrium shift of dehydrogenation at short space–time with hollow fiber ceramic membrane, *Ind. Eng. Chem. Res.* 30 (1991) 614–616.
- [21] T. Ioannides, G.R. Gavalas, Catalytic isobutene dehydrogenation in a dense silica membrane reactor, *J. Membr. Sci.* 77 (1993) 207–220.
- [22] N. Itoh, W.-C. Xu, K. Hayara, Basic experimental study on palladium membrane reactors, *J. Membr. Sci.* 66 (1992) 149–155.
- [23] P. Ciavarella, D. Casanave, H. Moueddeb, S. Miachon, K. Fiaty, J.-A. Dalmon, Isobutane dehydrogenation in a membrane reactor: influence of the operating conditions on the performance, *Catal. Today* 67 (2001) 177–184.
- [24] W.S. Moon, S.B. Park, Design guide of a membrane for a membrane reactor in terms of permeability and selectivity, *J. Membr. Sci.* 170 (2000) 43–51.
- [25] N. Itoh, K. Haraya, A carbon membrane reactor, *Catal. Today* 56 (2000) 103–111.